Designing of composite reticulated shell mounting for reflectors of satellite antennas enhanced ribs

Guo Jingyu[1*], *O.V.* Denisov [1], and *L.V.* Denisova[1]

[1]Bauman Moscow Technical University, ul. Baumanskaya 2-ya, 5/1, 105005 Moscow, Russia

Abstract. The growth in the number of communication satellites and the increase in antenna signal frequencies places higher demands on the accuracy and mass of reflectors. The accuracy of the reflector depends not only on its structure and materials but is also influenced by its mounting. In this paper, based on the rib-reinforced reflector designed by Bauman Moscow State Technical University, the effect of the reticulated shell mountings with different numbers of interlacing ribs in a shape of a circular truncated cone working in the geosynchronous orbit on the thermal deformation of the reflective surface is investigated by simulations using Siemens NX software. It is concluded that the desired deformation can be obtained when the number of t interlacing is 30. On thermal deformation, the effects of two weight reduction methods, namely reducing the width and thickness of ribs, were also investigated simultaneously. It is shown that reducing the thickness of ribs can achieve the target of mass reduction under the condition of ensuring the accuracy of the reflective surface. It is provided the basis for engineering calculations for practice.

1 Introduction

A growing number of countries and regions are researching and developing communication satellites to ensure the transmission of various types of information [1-3]. With an increase in the number of communication satellites, the signal frequency increases to 60 GHz and higher to provide the necessary amount of transmitted information [4,5]. Therefore, the requirements for the reflective surface precision of satellite mirror antennas are getting higher. The research shows that the deformation of the reflector should not exceed one-fiftieth of the wavelength of the antenna's reflected signal throughout the operation [6]. The deformation of the satellite mirror antennas' reflective surface is primarily generated by temperature uneven distribution due to the solar radiation and the reaction radiation from the Earth [7, 8].

To suppress the thermal deformation of reflective surfaces, new-type composite materials and structures were invented and created to fabricate satellite mirror antennas, in particular with the epoxy resin/carbon fiber, not merely because of its high specific modulus [9], but also because of its coefficient of thermal expansion in the direction along

* Corresponding author: denisov.sm13@mail.ru

the fiber less than one, therefore, through special design, the use of this material can achieve zero thermal expansion of the structure [10-11]. A more typical composite structure is the honeycomb interlayer structure, since the hexagonal honeycomb structure [12-14], which is perpendicular to the reflective surface, can effectively suppress the thermal deformation of the surface. For purpose of decreasing the mass of the satellite antennas, researchers designed and exploited a composite structure with enhanced ribs [15-21]. Although the principle of this structure is similar to the honeycomb interlayer structure, its manufacturing process is easier, the manufacturing cycle is shorter, and the weight is lighter.

The thermal deformation of the reflector depends not only on its material and structure but is also affected by its mounting. Currently, dual-gridded reflector design with reinforced stiffeners has become widespread [22]. The upper shell works as the reflective surface, and the lower shell links to the upper shell and the satellite. Another way is to use specially designed small brackets to connect the reflective surface back enhancement ribs to the satellite's main body [23]. Researchers at Bauman Moscow State Technical University designed a reticulated structure for connecting the satellite antenna to the satellite body, which can effectively reduce the thermal deformation of the reflective surface while controlling its mass [24]. However, the study has not fully discussed the reasons for the design of geometric parameters of the structure. Therefore, it is necessary to investigate the effect of the geometric parameters of the reticulated shell mounting on the performance of the mirror space antenna reflector.

2 Objects and materials

A reflector developed at the Bauman Moscow State Technical University was taken as a basic variant [1, 13, 25]. It was a paraboloid of rotation with an aperture of 1200 mm, a construction height of 180 mm and a focal length of 500 mm, reinforced with stiffeners according to the "six-pointed star" scheme (Fig 1). The expected frequency of the satellite antenna signal is at least 60 GHz, so the deflections of the reflector surface profile should not exceed 0.1 mm (Table 1).

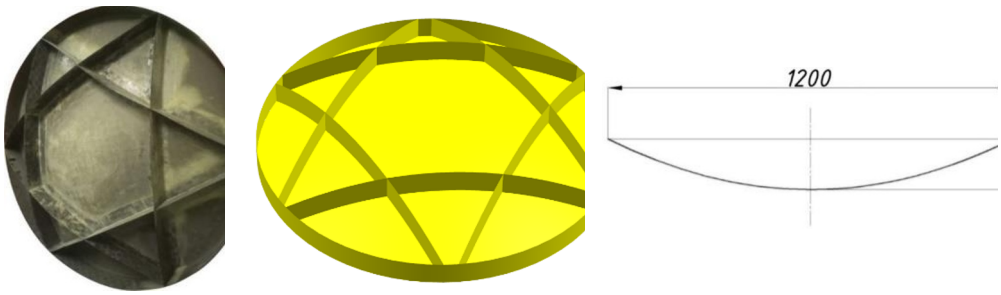

Fig. 1. Reflector of the mirror space antenna with composite six-manifold reinforcement ribs: a – photo of the full – scale reflector; b – 3D model of the reflector; c – profile of the reflecting surface

Table 1. Design parameters of the reflector

Rib thickness, mm	Shell thickness, mm	Rib height, mm	Reflector weight, kg	Maximum thermal deformation, mm	Linear density, kg/m^2

0.6	0.6	90	1.235	0.1	1.332

As a kind of reinforced composite structure, reticulated shell structure has been widely used in the aerospace field and has relatively mature manufacturing technology. However, it has not been used as a mounting for a satellite antenna. Therefore, the reticulated shell mounting with a height of 300 mm, a bottom radius of 320 mm, and a top radius of 150 mm was designed. The ring ribs are located in the middle of the intersection of the interlacing ribs. The baseline of the interlacing ribs that make up the grid is the geodesic line of that circular truncated cone.

It was assumed that the upper base of the mount is rigidly connected to the mate of the spacecraft with the help of fasteners, and the lower one is glued into the hexagon formed by the stiffening ribs of the reflector. The mesh mounting structure consists of annular and interlacing ribs. To increase the contact area and reduce the risk of rupture during the adhesive connection, special inserts are provided to increase the bonding area (Fig. 2).

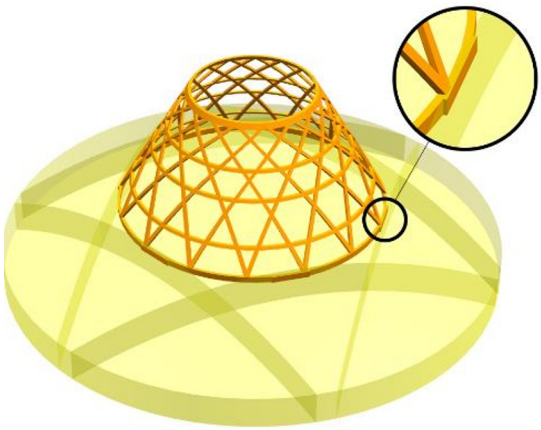

Fig. 2. Reflector mounting scheme

At the first stage of the design, the task was to determine the number of interlacing ribs at which the deformation of the surface profile is of the least importance. In the manufacture of mesh fastening, the width of the ribs is determined by the width of the prepreg used for winding and the width of the groove in the shape and is not subject to change at will. On the other hand, the thickness of the ribs can be changed depending on the number of layers of laying.

It was assumed that the mass of the considered mounting options, the number of ring elements and the width of the ribs had fixed values. Only the number and thickness of interlacing ribs varied. As a result, five variants of structures with different numbers of ribs were designed, as shown in Figure 3, and their specific parameters are shown in Table 2.

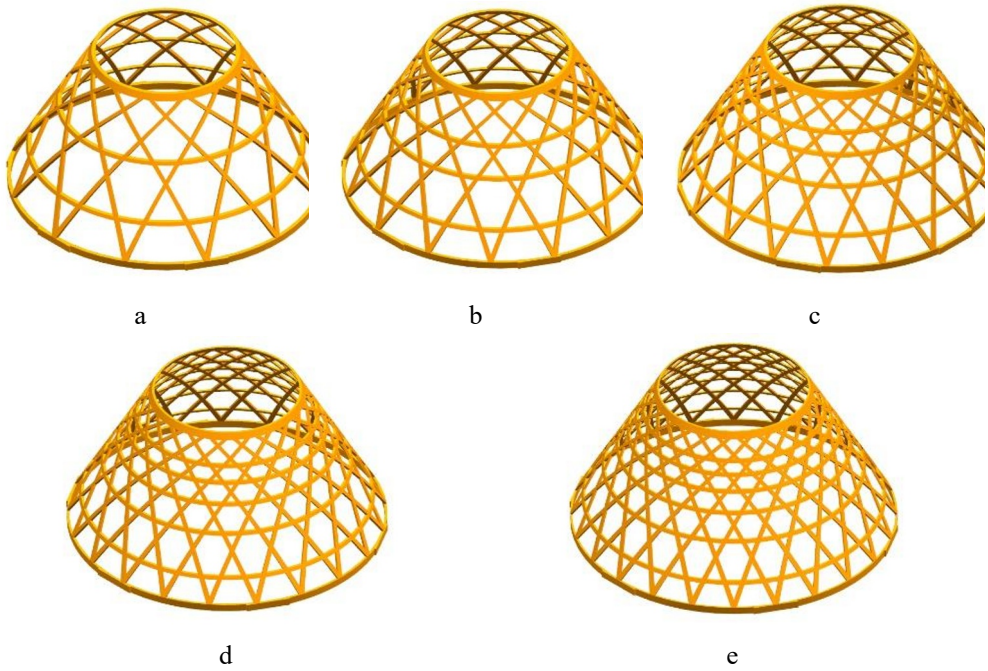

Fig. 3. Composite mesh structure mountings with different numbers N of the interlacing ribs: a – $N = 24$; b – $N = 30$; c – $N = 36$; d – $N = 42$; e – $N = 48$

Table 2. Parameters of mounting options

Design options	**a**	**b**	**c**	**d**
The number of the interlacing ribs N	24	30	36	42
The width of the interlacing ribs h , mm	8	8	8	8
The thickness of the ribs δ, mm	8.0	6.9	5.2	4.4

It was assumed that the reflector was made of quasi-isotropic carbon fiber reinforced plastic with a density of 1500 kg/m^3. The mounting material is isotropic. The parameters of the mechanical and thermophysical characteristics of the materials are given in Table 3.

Table 3. Parameters of reflector and mounting materials

Material properties	**Reflector**	**Mounting**
Young's modulus E, GPa E_1=E_2; E_3	 181.4 10.3	 140 140
Poisson ratio v: v_{12}=v_{13} v_{23}	 0.25 0.39	 0.3 0.3
Bending modulus G, GPa: G_{12}=G_{13}=G_{23}	6.9	6.9

Heat capacity C_p, J/(kg·K)	900	1000
Thermal expansion coefficient α, K^{-1}	0.5×10^{-6}	5.27×10^{-7}
Thermal conductivity λ, W/(m·K)	4	31
Emissivity ε	0.85	0.85
Absorbtivity A_S	0.735	0.735

3 Simulation

Simcenter 3D Space Systems Thermal solver in Siemens NX software was used to simulate the stress-strain state of the structure in geosynchronous orbit. It was assumed that the reflecting surface of the reflector is always directed at the Earth, and the direction of its movement is shown in Figure 5. The parameters of the environment in orbit are given in Table 4.

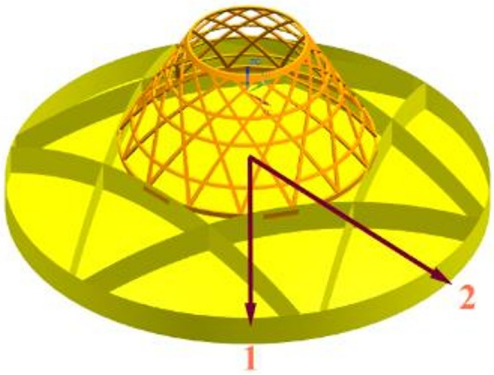

Fig. 4. In-orbit attitude of the structure: 1– pointing in the direction of the Earth; 2 – direction of the velocity vector

Table 1. Specific parameters of sampling points

The simulative albedo of Earth	0.306
The environmental temperature of the orbit, K	4
Solar Flux, W/m^2	
March Equinox	1377.8
June Solstice	1323.6
September Equinox	1357.3
December Solstice	1411.5

Eight sampling points equally distributed in the orbit are taken for the study, as shown in Fig. 6. The orbital times corresponding to the sampling points are shown in Table 5.

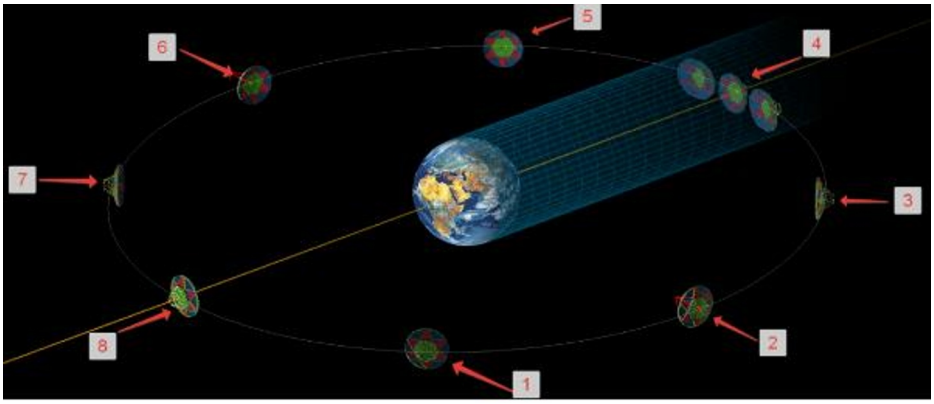

Fig. 5. Schematic diagram of the sampling points on the orbit

Table 5. Specific parameters of sampling points

Sampling points	1	2	3	4	5	6	7	8
Orbital time	10800	21600	32400	43200	54000	64800	75600	86400

The simulation results are shown in Table 6, including the maximum temperature difference and the moment when they occurred.

Table 6. Thermal calculation results of the structures

Design options	**Maximum temperature difference, K**	**Season time**	**Orbital time**
a	302.27	March Equinox	54000
b	233.55	December Solstice	21600
c	238.57	March Equinox	21600
d	247.16	December Solstice	64800
e	282.11	December Solstice	64800

Figure 7 shows the characteristic temperature deformations of the reflecting and lateral surfaces of the reflector. The greatest deformations are observed on the lateral surface, but it does not participate in the reflection of the signal. Therefore, in the further analysis, only the reflecting parabolic surface of the reflector will be considered.

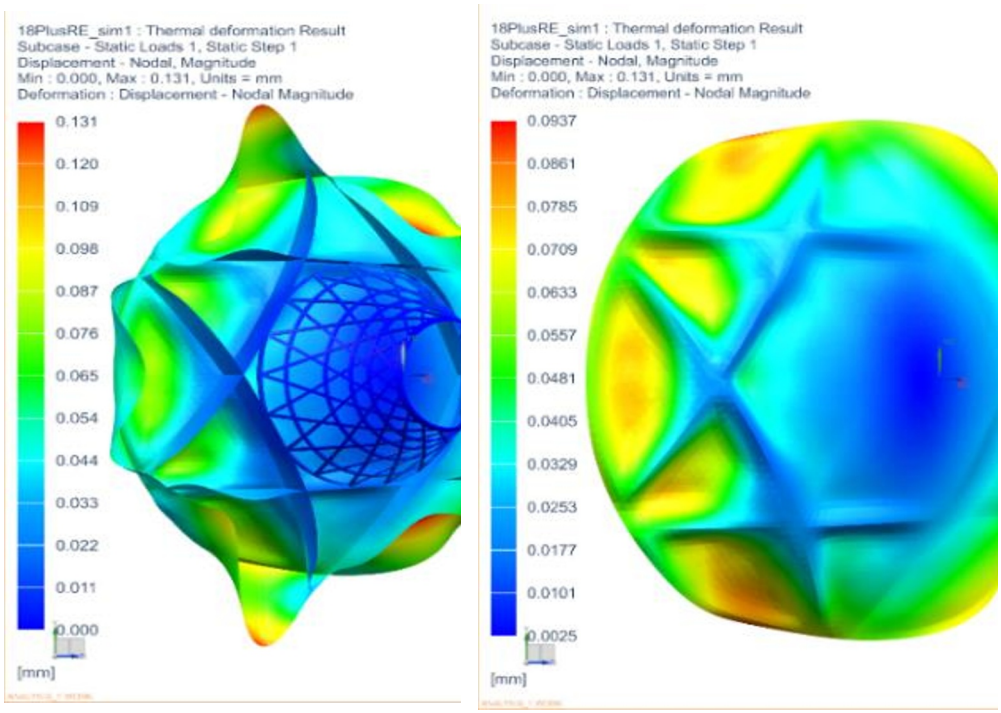

a b

Fig. 6. Thermal deformation of the structure: a – the whole structure; b – reflective surface (scale factor 10)

By counting the obtained thermal deformation data, the maximum deformation at different periods was obtained as shown in Table 7.

Table 7. Thermal deformation calculation results of the structures

Design options	March Equinox Δ, mm	June Solstice Δ, mm	September Equinox Δ, mm	December Solstice Δ, mm
a	0.118	0.088	0.118	0.089
b	0.083	0.071	0.083	0.072
c	0.094	0.077	0.094	0.071
d	0.087	0.082	0.087	0.084
e	0.118	0.094	0.117	0.095

It can be concluded from the table that the maximum deformation tends to occur in the spring and autumn equinox. It is assumed that the design retains dimensional stability if the maximum thermal deformation of the reflecting surface of the reflector does not exceed the permissible values. For modern reflectors, the maximum profile deviations should not exceed 0.1 mm. With the number of spiral ribs 30, the maximum deformation is no more than 0.083 mm, which satisfies this requirement.

Figure 8 shows the relationship between the root-mean-square (RMS) value of the displacements of the reflecting surface and the orbital time. The greatest profile deviations

occur at the moments corresponding to characteristic points 2, 4 and 6, when the direction of movement of the satellite antenna is parallel to the direction of solar radiation and when it is in the shadow of the Earth. The areas covered by the curves show the degree of thermal deformation of the reflecting surface. The larger the area bounded by the curves, the greater the thermal deformation.

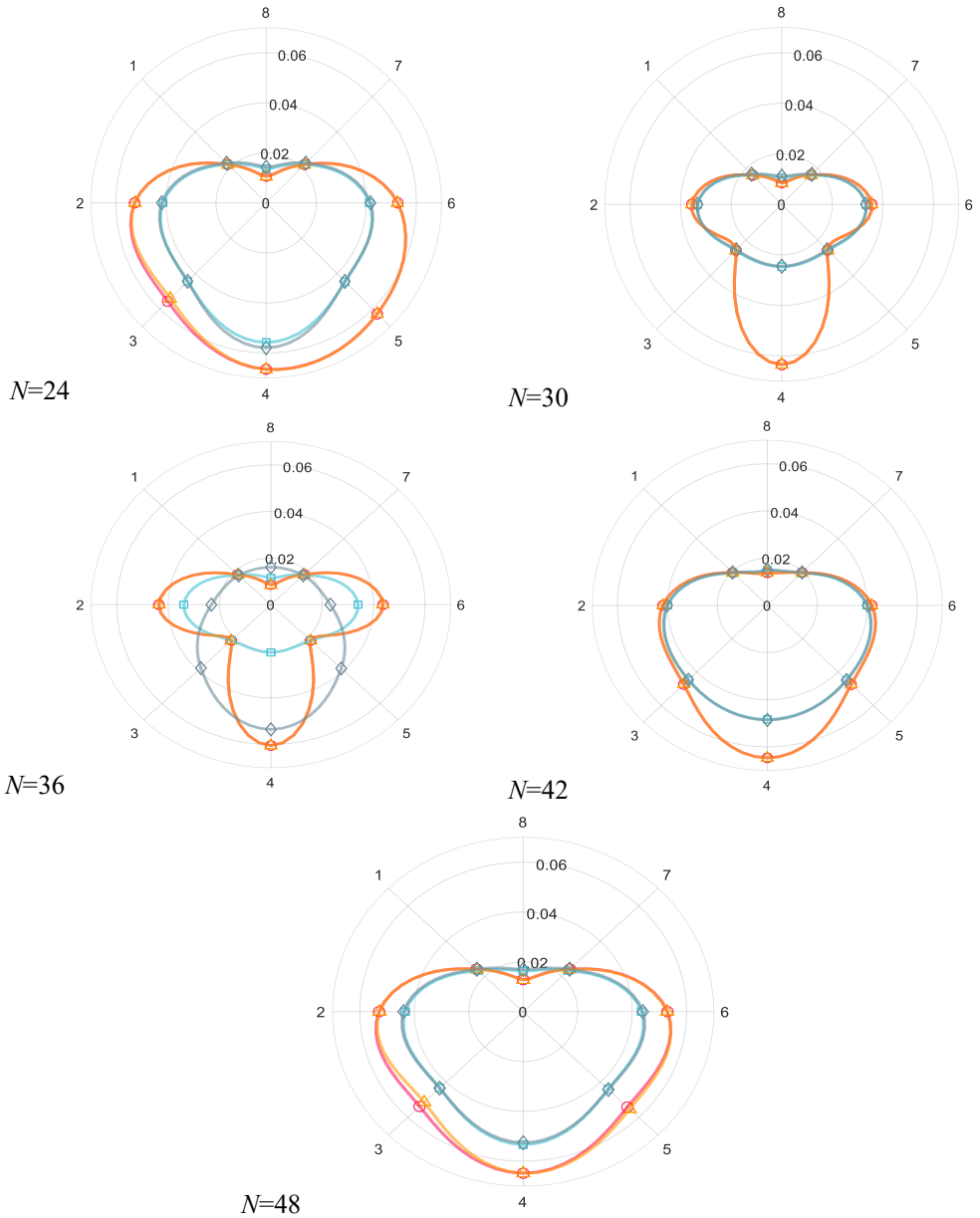

Fig. 1. RMS of the thermal deformation on the reflective surface of the structures with different interlacing ribs in different seasons: Rose red circle – march equinox; Cyan square – june solstice; Orange-yellow – september equinox; Green rhombus – december solstice

Of the options considered, the most rational is a mount with 30 interlacing ribs (Fig. 9).

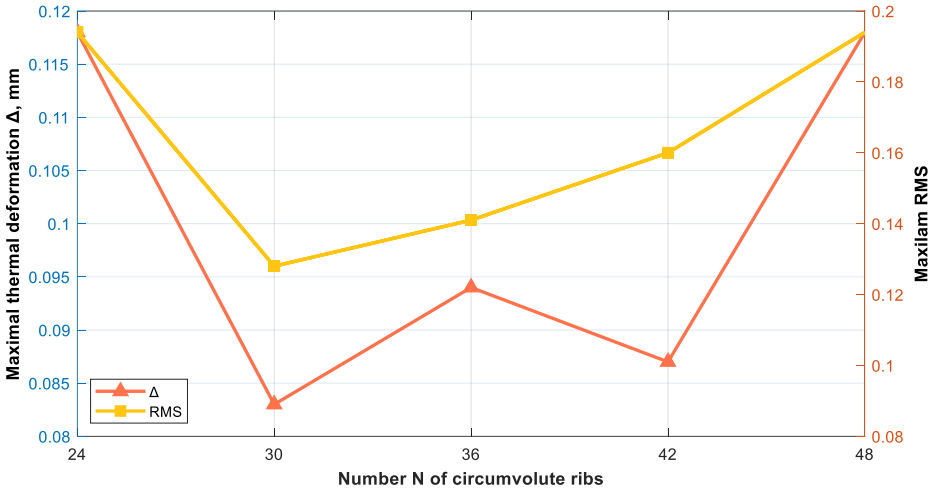

Fig. 2. Relationship between thermal deformation and the number of interlacing ribs

The mass of the mounting can be reduced by reducing the cross-sectional area of the ribs. At the second stage, the effect of the size of the ribs on the deformation of the reflecting surface of the reflector is investigated. For a structure with 30 interlacing ribs, options are considered in which the width and thickness of the ribs are reduced by two times, respectively, relative to the base dimensions. Reducing the thickness of the ribs has a less active effect on the deformation of the reflecting surface of the reflector (Fig. 10 and Table 8).

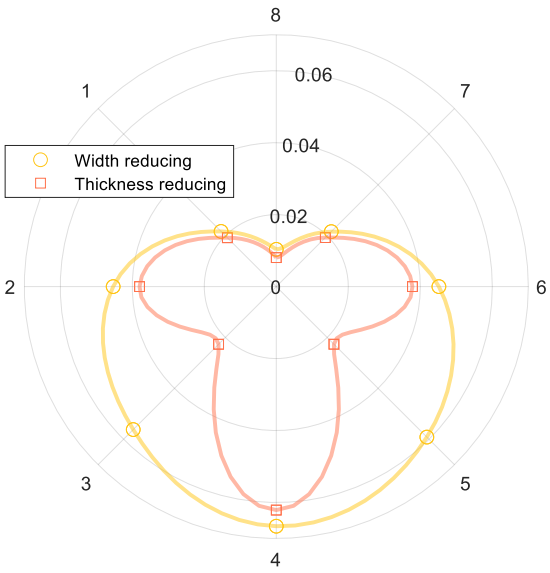

Fig. 3. RMS of the thermal deformation of the reflective surface after weight reducing

Table 8. Thermal deformation of the structure after weight reduction

Thermal deformation, mm	Basic variation h = 8 mm, δ = 6.9 mm	Width reducing variation $h/2$ = 4 mm,	Thickness reducing variation h = 8 mm, δ/2 = 3.5

		δ = 6.9 mm	**mm**
Δ_{max}	0,083	0,110	0,088

From the graphs and tables, the thickness-reducing variation results in a smaller maximum thermal deformation and a smaller RMS value of the reflective surface. Therefore, for the weight reduction design, it is reasonable to reduce the thickness of the ribs.

4 Conclusions

Variants of the shell mounting of the satellite antenna reflector in the form of a truncated cone of interlacing and annular ribs with high dimensional stability are proposed. The most rational is a mount with 30 spiral stiffeners, which ensures temperature movements of the reflecting surface of the reflector in a geostationary orbit of no more than 0.1 mm. It was found that in order to reduce the weight of the mount, it is advisable to reduce the thickness of the mesh shell ribs.

References

1. S. V. Reznik, A. D. Novikov, Comparative analysis of the honeycomb and thin-shell space antenna reflectors (2016) https://doi.org/10.1051/matecconf/20179201012
2. S. Ren, X. Yang, R. Wang, S. Liu, X. Sun, The interaction between the LEO satellite constellation and the space debris environment, Applied Sciences (Switzerland), 11 (2021) https://doi.org/10.3390/app11209490
3. F. Appaix, C. Boddaert, K. Bellido, L. Hobbs, EUTELSAT 2 FM4 spacecraft end of life operations and propulsion passivation, 75-85 (2004)
4. S. H. Dole, The gravitational concentration of particles in space near the earth, Planetary and Space Science, **9**, 541-553 (1962) https://doi.org/10.1016/0032-0633(62)90040-5
5. D. Sagar, Inmarsat Inmarsat and the Mariner, The International Journal of Marine and Coastal Law., 14 (1999) https://doi.org/10.1163/15718089920492519.
6. P. V. Prosuntsov, S. V. Reznik, K. V. Mikhailovsky, A. D. Novikov, Z. Y. Aung, Study variants of hard CFRP reflector for intersatellite communication, IOP Conf. Series: Materials Science and Engineering, **153**, 012012 (2016) https://doi.org/10.1088/1757-899X/153/1/012012
7. J. D. Johnston, E. A. Thornton, Evaluation of thermally-induced structural disturbances of spacecraft solar arrays, 1-6 (1996)
8. M. Xue, Y. Ding, Two kinds of tube elements for transient thermal-structural analysis of large space structures International Journal for Numerical Methods in Engineering. **59**. 1335-1353 (2004) https://doi.org/10.1002/nme.918
9. H. Tian, Z. Guan, Y. Ding, K. Wu, Carbon fiber composite material applied to aerospace optical remote sensor shading lens barrel, Optical Technique, 704-706 (2003) https://kns.cnki.net/kns8/Detail?sfield=fn&QueryID=2&CurRec=10&recid=&FileNam

e=GXJS200306021&DbName=CJFD2003&DbCode=CJFD&yx=&pr=&URLID= (Last accessed October 30, 2022).

10. D. Yang, L. Yao, H. Mei, S. Zhou, Y. Tan, L. Cheng, L. Zhang, Near-zero expansion of ceramics by 3D printing thermally induced torsional structures Materials Letters, **305**, 130836 (2021) https://doi.org/10.1016/j.matlet.2021.130836
11. X. Pang, Y. Song, N. Shi, M. Xu, C. Zhou, J. Chen, Design of zero thermal expansion and high thermal conductivity in machinable xLFCS/Cu metal matrix composites, Composites Part B: Engineering, **238**, 109883 (2022) https://doi.org/10.1016/j.compositesb.2022.109883
12. Y. Arao, J. Koyanagi, S. Utsunomiya, H. Kawada, Analysis of thermal deformation on a honeycomb sandwich CFRP mirror Mechanics of Advanced Materials and Structures, **17**, 328 - 334 (2010) https://doi.org/10.1080/15376494.2010.488533
13. S. V. Reznik, P. V. Prosuntsov, A. D. Novikov, Prospects of Increasing the Dimensional Stability and the Weight Efficiency of Mirror Space Antenna Reflectors Made of Composite Materials BMSTU Journal of Mechanical Engineeringpp, 71-83 (2018) https://doi.org/10.18698/0536-1044-2018-1-71-83
14. Reflector Antennas, HPS GmbH – The Team to Trust. (n.d.). https://www.hps-gmbh.com/en/portfolio/subsystems/reflector-antennas/ (Last accessed October 27, 2022).
15. Baunge M., Ekström H., Ingvarson P., Petersson M., A new concept for dual gridded reflectors Proceedings of the Fourth European Conference on Antennas and Propagation, 1 - 5 (2010)
16. H.-Y. Lee, The design of high gain waveguide array antenna combining horn antenna Transactions of the Korean Institute of Electrical Engineers, **63**, 257-260 (2014) https://doi.org/10.5370/KIEE.2014.63.2.257
17. L. Datashvili, S. Endler, B. Wei, H. Baier, H. Langer, M. Friemel, N. Tsignadze, J. Santiago-Prowald, Study of mechanical architectures of large deployable space antenna apertures: From design to tests CEAS Space Journal, **5**, 169–184 (2013) https://doi.org/10.1007/s12567-013-0050-9
18. Y. Rahmat-Samii, R. Haupt, Reflector Antenna Developments: A Perspective on the Past, Present and Future IEEE Antennas and Propagation Magazine, **57**, 85-95 (2015) https://doi.org/10.1109/MAP.2015.2414534
19. R. Zhang, X. Guo, Y. Liu, J. Leng, Theoretical analysis and experiments of a space deployable truss structure Composite Structures, **112**, 226-230 (2014) https://doi.org/10.1016/j.compstruct.2014.02.018
20. C. Liu, Y. Shi, Comprehensive structural analysis and optimization of the electrostatic forming membrane reflector deployable antenna Aerospace Science and Technology, **53**, 267 - 279 (2016) https://doi.org/10.1016/j.ast.2016.03.026
21. H. Tanaka, Study on a Calibration Method for Shape Control Parameters of a Self-Sensing Reflector Antenna Equipped with Surface Adjustment Mechanisms Transactions of the Japan Society for Aeronautical and Space Sciences, **57**, 86-92 (2014) https://doi.org/10.2322/tjsass.57.86
22. M. Baunge, H. Ekstrom, P. Ingravson, M. Petersson, A new concept for dual gridded reflectors Proceedings of the Fourth European Conference on Antennas and Propagation, 1-5, (2010) https://ieeexplore.ieee.org/document/5505375 (Last accessed October 31, 2022)
23. A. U. Vlasov, M. V. Serzhantova, Ya. A. Andreeva, Innovative technology of products made of composite materials in the resource centre «Spacecraft and systems» SibSAU

Spacecrafts & Technologies, 8-12 (2016) http://journal-niss.ru/en/archive_view.php?num=116 (Last accessed October 31, 2022).

24. A. V. Belyaeva, O. V. Denisov, Designing of Space Antenna Mounting XLIV ACADEMIC SPACE CONFERENCE: dedicated to the memory of academician S.P. Korolev and other outstanding Russian scientists – Pioneers of Space Exploration, **1**, 76-78 (2020)
25. P. V. Prosuntsov, S. V. Reznik, K. V. Mikhailovsky, A. D. Novikov, Z. Y. Aung, Study variants of hard CFRP reflector for intersatellite communication. IOP Conf. Series: Materials Science and Engineering, **153(1)**, 012012 DOI:10.1088/1757-899X/153/1/012012